RSC Advances

ROYAL SOCIETY OF CHEMISTRY

www.rsc.org/advances

Insights into the Mechanism and Kinetics for Gas-phase Atmospheric Reaction of 9-Chloroanthracene with NO_3 Radical in the Presence of NO_X

Juan Dang, Xiangli Shi, Qingzhu Zhang*, Jingtian Hu, Wenxing Wang

Environment Research Institute, Shandong University,

Jinan 250100, P. R. China

*Corresponding author. E-mail: zqz@sdu.edu.cn

Fax: 86-531-8836 1990

Abstract

9-chloroanthracene (9-ClAnt), an important member of chlorinated polycyclic aromatic hydrocarbons (ClPAHs), has been demonstrated to show strong direct mutagenic effects. To elucidate the chemical transformations, degradation products and the capacity to undergo long-range transport of 9-ClAnt in the atmosphere, we conducted a theoretical investigation on the oxidation mechanism and kinetics of the NO_3-initiated atmospheric transformation of 9-ClAnt by using quantum chemistry method. The rate constants for the crucial elementary reactions were also estimated. The main oxidation products for the gas-phase reactions of 9-ClAnt with NO_3 radicals include 9-chloroanthracen-yl nitrates, 9-chloroanthracenesdiones, epoxides, dialdehydes, 9-chloroanthracene-1,4-dione, anthracene-9,10-dione, 9-chloroanthracen-1-one, 10-chloroanthracen-1-one, 10-chloroanthracen-9-ol and 10-chloro-1-nitroanthracene etc. The overall rate constant of the NO_3 addition reactions is 9.11×10^{-13} cm^3 $molecule^{-1}$ s^{-1} at 298 K and 1atm. The atmospheric lifetime of 9-ClAnt determined by NO_3 radicals is about 0.61 hr. This comprehensive investigation is the first report for the NO_3-initiated oxidation of ClPAHs in the atmosphere. It should be conducive to clarifying their atmospheric fates and developing a full understanding of their toxic potential.

Keywords: 9-chloroanthracene, NO_3 radicals, Oxidation mechanism, Degradation products, Rate constants

1. Introduction

Chlorinated polycyclic aromatic hydrocarbons (ClPAHs) have attracted considerable interest because of their ubiquitous presence in the environmental matrices and potential dioxin-like toxicity.[1-4] ClPAHs can elicit toxic effects via hindering the function of the aryl hydrocarbon receptor (AhR).[5] Automobile exhaust and municipal incineration have been perceived as major emission sources of ClPAHs.[6] Compared with their parent polycyclic aromatic hydrocarbons (PAHs), ClPAHs have lower vapor pressures, higher octanol-water partition coefficient values, and even possess stronger mutagenicity and toxic effects.[4,7] ClPAHs have been constantly detected in the atmosphere and the concentration in urban air was up to 143 pg m^{-3} in Japan.[8] Due to the scarcity of purified individual ClPAHs standards, the environmental behavior and fate of these compounds in the atmosphere have not been fully clarified.

9-chloroanthracene (9-ClAnt), a chloro-substituted anthracene derivative, has been demonstrated to show strong direct mutagenic effects.[9, 10] According to the report, 9-ClAnt has been frequently detected in the atmospheric monitoring. In December 2009, air samples collected from the urban area of Shizuoka in Japan showed that the maximum concentration of 9-ClAnt was 12.10 pg m^{-3}.[11] The measurement in a Japanese urban city from December 2004 to December 2005 indicated that ambient air concentrations of 9-ClAnt ranged from $<$0.02 to 71 pg m^{-3}.[12] Given its toxicity and prevalent presence in air, little is known about the

atmospheric fate of 9-ClAnt.

Under typical ambient conditions, 9-ClAnt exists mainly in the gas phase and can be removed from the atmosphere by gas-phase reactions with OH radicals, NO_3 radicals and O_3.[7, 13] The reaction with OH radicals is an important loss process during daylight hours, and reaction with NO_3 radicals is dominant chemical transformations during the evening and nighttime.[13] Compared to the reaction with OH, the reaction of PAHs with NO_3 appears to be less significant. However, considering the higher yields of nitro-PAH in the nighttime, it suggests that the reaction with NO_3 may also play an important role.[14] To date, no information on the NO_3-initiated atmospheric oxidation of ClPAHs (9-ClAnt included) is available in previous studies. Besides, a complete analysis of the atmospheric reactions is limited in the laboratory studies, largely due to the lack of efficient detection schemes for intermediate radical species. Hence we carried out a comprehensive theoretical investigation on the NO_3-initiated atmospheric oxidation of 9-ClAnt in the presence of O_2/NO_x, using the quantum chemistry calculation and the energy grained master equation.[15-17] The reaction mechanisms of the NO_3-initiated atmospheric oxidation of 9-ClAnt and the rate constants for the key elementary reactions were obtained.

2. Computational Method

The electronic structure calculations were performed with the Gaussian 09 software program suite.[18] The hybrid density functional theory (DFT), BB1K, can

give excellent transition state geometries and barrier heights, based on Becke's 1988 gradient corrected exchange functional (Becke88 or B) and Becke's 1995 kinetic-energy-dependent dynamical correlation functional (Becke95 or B95).[19] Truhlar et al indicated that the hybrid DFT results are much less sensitive to the basis set compared to the ab initio ones, and they also emphasized the importance of diffuse functions. [20, 21] According to the assessment of different methods by Zheng et al., the mean signed errors and mean unsigned errors for the DBH24/08 database as well as the errors for its components: heavy-atom transfer (HATBH6), nucleophilic substitution (NSBH6), unimolecular and association (UABH6), and hydrogen-transfer (HTBH6) reactions indicated that BB1K/ 6-31+G(d,p) have a comparatively high accuracy [22]. Therefore geometries of the reactants, intermediates, transition states, and products were optimized at the BB1K/6-31+G(d,p) level. The transition states were identified with one imaginary frequency. The harmonic frequencies calculations were also performed at the same level in order to determine the character of the stationary points, the zero-point energy (ZPE), and the thermal contribution to the free energy of activation. Besides, the intrinsic reaction coordinate (IRC) analysis was executed to confirm that each transition state connects to the right minima along the reaction path. For a more accurate evaluation of the energetic parameters, a more flexible basis set 6-311+G(3df,2p), was employed to determine the single point energies of various species. The profile of the potential energy surface (PES) was constructed at the BB1K/6-311+G(3df,2p)//BB1K/6-31G+G(d,p) level. All the total electronic energies were corrected by the zero-point energy.

All calculations for the rate constants have been performed by means of the MESMER program,[17] MESMER uses matrix techniques to formulate and solve the energy grained master equation (EGME) for unimolecular systems. The exponential down model is used for describing collisional energy transfer probabilities. The expression is: [23]

$$P(E \leftarrow E') = C(E')\exp\left[-\frac{E'-E}{\langle \Delta E_d \rangle}\right] \quad (1)$$

where $E' > E$, $C(E')$ is a normalization constant, and $\langle \Delta E_d \rangle$ is the average energy transferred per collision in a downward direction.

The population distribution of the reactants and intermediates on the potential energy surface (PES) was calculated by solving coupled differential equations that depict collisional energy transfer and interconversion between the species.[24-26] The coupled set of differential equations may be expressed as:

$$\frac{d}{dt}\mathbf{p} = \mathbf{M}\mathbf{p} \quad (2)$$

Where **p** is the population vector including the populations of the energy grains for each isomer and **M** is the matrix describing population evolution due to collisional energy transfer and reaction.

For unimolecular reactions with a well-defined transition state, the most common way of obtaining energy resolved microcanonical rate constants for a particular energy grain, $k(E)$, were determined by using Rice-Ramsperger-Kassel-Marcus (RRKM) theory. The RRKM expression is given by: [24]

$$k(E) = \frac{W(E - E_0)}{h\rho(E)} \quad (3)$$

Where $W(E\text{-}E_0)$ is the rovibrational sum of states at the transition state, E_0 is the reaction threshold energy, $\rho(E)$ is the density of rovibrational states of reactants, and h is Planck's constant.

If no transition state is specified, an inverse Laplace transform (ILT) offers a mathematical formalism for deriving $k(E)$s from an Arrhenius fit to a set of $k(E)$s. The basis of the ILT is the standard (high-pressure limit) Boltzmann average which may be expressed as:[24]

$$k^{\infty}(\beta) = \frac{1}{Q(\beta)} \int_0^{\infty} k(E)\rho(E)\exp(-\beta E)dE \quad (4)$$

Where $Q(\beta)$ is the corresponding canonical partition function and $\rho(E)$ is the reactant rovibrational density of states. Then representing $k^{\infty}(\beta)$ by an modified Arrenhius expression can obtain $k(E)$ as an ILT.

For a barrierless association reaction, considering the reverse unimolecular dissociation of the collision adduct, the forward (association) and reverse (dissociation) rate constants are related by the equilibrium constant. So the rate constant of the forward (association) reaction can be derived from the equilibrium constant and the rate constant of the reverse (dissociation) reaction. [24]

3. Results and Discussion

3.1 Reaction with NO_3 Radicals

As shown in Figure 1 and Figure S1 (Supporting Information), the carbon

atoms in the molecular of 9-ClAnt are numbered. Addition of NO_3 to the C=C bonds and H abstraction from the C-H bonds by NO_3 radicals are possible pathways for the reaction of 9-ClAnt with NO_3 radicals. At the BB1K/6-311+G(3df,2p) level, the potential barriers of H abstractions are 39.33~57.78 kJ/mol and all reaction channels are endothermic by 31.00~36.19 kJ/mol. The geometrical structures of the transition states for the H abstractions by NO_3 radicals are shown in Figure S4. For the NO_3 additions, the reactions are barrierless and the reaction heats are from -62.17 to -113.59 kJ/mol. Clearly, the NO_3 additions are the energetically more favorable reaction pathways for the reaction of 9-ClAnt with NO_3 radicals, which is consistent with the previous investigations of the NO_3-initiated atmospheric oxidations of unsubstituted PAHs.[27,28] The NO_3 addition reactions lead to the formation of NO_3-9-ClAnt adducts.

3.2 Secondary Reactions

3.2.1 Reactions with O_2

The NO_3-9-ClAnt adducts generated from the reaction of 9-ClAnt with NO_3 radicals can further react with O_2/NO_x as their removal. The reaction schemes embedded with the potential barriers ($\triangle E$) and reaction heats ($\triangle H$, 0K) are presented in Figure 2. For IM1, the H abstraction by O_2 lead to the formation of 9-chloroanthracen-1-yl nitrate (P1). The potential barrier of this process is 85.60 kJ/mol at the BB1K/6-311+G(3df,2p) level and the process is exothermic by 25.86

kJ/mol. P1 can further proceed with NO_2 shift from C1atom to the adjacent C2 atom to yield the intermediate IM7. This elementary reaction is the rate-determining step because of the high barrier of 116.19 kJ/mol. The subsequent reaction of IM7 involves H abstraction by O_2 and elimination of NO, both of which are easily to occur under general atmospheric conditions. It ultimately result in the generation of 9-chloroanthracene-1,2-dione (P6). Similar to IM1, IM2, IM3 and IM4 also can undertake these reactions to yield 9-chloroanthracen-yl nitrates and 9-chloroanthracenesdiones. Furthermore, as shown in Figure S2, the NO_3-9-ClAnt adducts may proceed with NO_2 migration, H shift and H abstraction by O_2 to form nitroanthracenones and nitroanthracenols. For instance, 1-nitroanthracen-2-one and 1-nitroanthracen-2-ol could be the products of these processes. The process of H shift is the rate-determining step due to its high barrier.

The NO_3-9ClAnt adducts are resonantly stabilized radicals. According to the nodal pattern of the Hückel theory, the single occupied molecular orbital (SOMO) for the NO_3-9ClAnt adduct only has combinations on the ortho- or para-positions of $-NO_3$ moiety. As depicted in Figure 3, for IM1, O_2 can attack the C atoms from the *ortho*- and *para*-positions of nitryl to produce two O_2-NO_3-9-ClAnt adducts (IM15 and IM19). The sequential reaction of IM15 contains four processes: NO barrierless association, elimination of NO_2, cleavage of the C-C bond and loss of NO_2. Thereinto, the formation of IM17 is the rate-determining step with a high potential barrier of 199.11 kJ/mol. A dialdehyde (P8) is formed from these reactions. Analogous products dialdehydes have been detected in the simulation chamber experiments of gas-phase

atmospheric oxidation of acenaphthylene with NO_3 radicals.[29] The subsequent reaction of IM19 starts with NO addition, followed by elimination of NO_2, H abstraction by O_2, H abstraction by OH radical and loss of NO_2, leading to the formation of 9-chloroanthracene-1,4-dione (P11). The calculated profile of the potential energy surface shows that the step of the O-ONO bond cleavage is difficult to occur because of the high potential barrier of 191.58 kJ/mol. IM2 also can react with O_2, proceeding with NO addition, cleavage of the O-ONO bond, C-C bond rupture and elimination of NO_2, and it ultimately results in the formation of a dialdehyde (P8). The subsequent reaction from IM6 includes six elementary reactions: O_2 addition, NO addition, O-ONO bond fission, elimination of Cl, H abstraction by OH radical and elimination of NO_2, which lead to the generation of anthracene-9,10-dione (P12).

3.2.2 Unimolecular Decomposition

The NO_3-9-ClAnt adducts also can undertake unimolecular decompositions, yielding epoxides and dialdehydes. As shown in Figure S3, one-step reactions can lead to the generation of epoxides via the loss of NO_2. The potential barriers for the formation of epoxides range from 103.93 kJ/mol to 139.83 kJ/mol. As presented in Figure 4, another decomposition channel of IM1 initiates from the isomerization to IM33, leading to the generation of a five-membered ring. The barrier height is calculated to be 115.77 kJ/mol, and the process is endothermic by 24.18 kJ/mol. There

exist two kinds of the five-membered ring opening via two different N-O bonds rupture, which produce two intermediates IM34 and IM36. The subsequent reactions of IM34 and IM36 are cleavage of the C-C bonds and elimination of NO, both of which are easily to proceed under general atmospheric conditions. A dialdehyde (denoted as P8) is ultimately formed. Another NO_3-9-ClAnt adduct, IM3, also can proceed with these processes via a similar mechanism of IM1, which produce a dialdehyde (P9). As presented, the unimolecular decomposition pathway of IM6 may be difficult to proceed because of the high potential barrier and large endothermicity. The reaction schemes of IM2 and IM4 are depicted in Figure S3. IM2 and IM4 can isomerize to five-membered rings, and followed by ring-opening reactions and unimolecular decomposition.

As shown in Figure 5, IM1 can undergo cyclization to produce the intermediate IM48. The subsequent reactions from IM48 are two different N-O bonds fissions and result in the formation of IM49 and IM52. Then, 9-chloroanthracen-1-one (P13) and 10-chloroanthracen-1-one (P14) can be formed from the subsequent reactions of IM52 and IM49 through NO_2 elimination, respectively. Another reaction channel of IM49 includes H abstraction by O_2, H abstraction by OH radical and loss of NO with a rearrangement, which lead to the formation of 9-chloroanthracene-1,4-dione (P11). Calculations show that the formation of the intermediate IM48 is the rate-determining step due to its high potential barrier. Similarly, IM6 also can proceed with isomerization to form IM53, followed by cleavage of the N-O bond and rearrangement. The intermediate IM55 is generated

from these processes. Subsequently, 10-chloroanthracen-9-ol (P15) can be formed by IM55 through loss of NO_2. Another reaction pathway of IM55 contains two elementary reactions: elimination of ClNO and H abstraction by O_2, which yield anthracene-9,10-dione (P12). Similar products, 1,4-naphthoquinone, have been detected in the experimental studies of the reaction of naphthalene with NO_3 radicals.[27] Calculations show that both of the two pathways are the energetically favorable processes for the further reactions of IM55.

3.2.3 Reactions with NO_2

The reaction schemes for the NO_3-9-ClAnt adduct and NO_2 are presented in Figure 6. IM1 can react with NO_2 via a barrierless addition to form the intermediate IM57. The energy of IM57 is 136.36 kJ/mol lower than the total energy of IM1 and NO_2. The subsequent reaction of IM57 proceeds either by elimination of HONO or by loss of HNO_3, which lead to the formation of 9-chloroanthracen-1-yl nitrate (P1) and 9-chloro-2-nitroanthracene (P16). The potential barrier for the formation of P1 is 164.14 kJ/mol, and the process is exothermic by 7.74 kJ/mol. The barrier height of the formation of P16 is 179.78 kJ/mol, and the reaction enthalpy is -49.45 kJ/mol, which indicate it may be difficult to occur under typical atmospheric conditions. IM2, IM3 and IM4 also can react with NO_2 and produce 9-chloroanthracen-yl nitrates and 9-chloronitroanthracenes. By comparison, the generation of 10-chloro-1-nitroanthracene (P18) from the intermediate IM59 is more favorable than

other formation pathways of P16, P17 and P19. The barrier height and reaction enthalpy for the formation of P18 is 134.22 kJ/mol and -31.04 kJ/mol, respectively. Similar products (1- and 2-nitronaphthalene) have been detected in the experiment of the reaction of naphthalene with NO_3 radicals.[30]

3.2.4 Comparisons with Reactions of 9,10-dichlorophenanthrene with OH Radicals

The reaction of ClPAHs with OH radicals also plays an import role in the atmosphere. According to our previous study, the OH-initiated atmospheric oxidation of 9,10-dichlorophenanthrene (9,10-diClPhe) also generates a class of ring-retaining and ring-opening products containing chlorophenanthrols, 9,10-dichlorophenanthrene-3,4-dione, dialdehydes, chlorophenanthrenequinones, nitro-9,10-dichlorophenanthrenes and epoxides,[31] which are similar to that of the reaction with NO_3. However their reaction mechanisms have significant differences, for instance, the NO_3-9-ClAnt adducts can undertake unimolecular decompositions to produce dialdehydes, but OH-9,10-dichlorophenanthrene adducts have no analogous reactions. The reactions of the NO_3-9-ClAnt adducts with NO_2 are also different from that of OH-9,10-diClPhe adducts with NO_2.

3.3 Rate Constant Calculations

The rate constants for the critical elementary reactions involved in the NO_3-initiated atmospheric reactions of 9-ClAnt were estimated by using the MESMER program. [17] The MESMER program has been successfully applied to calculate the rate constants of many reactions.[24, 26] For the elementary reactions with well-defined transition states, the SimpleRRKM method was used to obtain the rate constants at 298 K and 1 atm, while the MesmerILT method was applied to calculate the rate coefficients for the barrierless reactions at 298 K and 1atm. As shown in the Table 1, the individual rate constants for the NO_3 addition to the C_1-H, C_2-H, C_3-H, C_4-H, C_9-H and C_{10}-H bonds of 9-ClAnt are denoted as k_1, k_2, k_3, k_4, k_5, k_6, respectively. Considering the structural symmetry of 9-ClAnt, the overall rate constant of the NO_3 addition reactions is denoted as k, $k=(k_1+k_2+k_3+k_4)\times2+k_5+k_6$. The overall rate constant k is calculated to be 9.11×10^{-13} cm^3 $molecule^{-1}$ s^{-1} at 298 K and 1atm. The rate constants of the crucial secondary reactions of NO_3-9-ClAnt adducts were also calculated, which can be helpful to the establishment of the kinetic models describing the atmospheric fate of 9-ClAnt. From the Table 1, it can be clearly observed that the formation of 10-chloro-1-nitroanthracene (P18) from IM59 is much easier than the generation of 9-chloro-2-nitroanthracene (P16) from IM57.

The atmospheric lifetime of 9-ClAnt determined by NO_3 can be derived from the overall rate constant (k) of the NO_3 addition reactions and the NO_3 concentration ($[NO_3]$). An average 12 h nighttime value for NO_3 concentration in the low troposphere is approximately 5.0×10^8 molecule cm^{-3},[29] from the

expressions: $\tau = \frac{1}{k\,[NO_3]}$, the atmospheric lifetime (τ) of 9-ClAnt determined by NO_3 is calculated to be 0.61 hr, which indicate that 9-ClAnt can be removed from the atmosphere quickly and have less potential to undergo long-range transport to remote areas.

4. Conclusions and Environmental Perspectives

In this work, we conducted an extensive theoretical study on the reaction mechanism and kinetics of the NO_3 radical-initiated atmospheric oxidation of 9-ClAnt. The rate constants for the crucial elementary reactions were evaluated by using the MESMER program. The following specific conclusions can be summarized from this study:

(1) Compared with H abstractions by NO_3 radicals, the NO_3 additions are the energetically more favorable reaction pathways for the reaction of 9-ClAnt with NO_3 radicals. The NO_3 addition reactions are barrierless and the reaction heats range from -62.17 to -113.59 kJ/mol.

(2) The NO_3-initiated atmospheric oxidation of 9-ClAnt generates a class of anthracene derivatives containing 9-chloroanthracen-yl nitrates, 9-chloroanthracenesdiones, epoxides, dialdehydes, 9-chloroanthracene-1,4-dione, anthracene-9,10-dione, 9-chloroanthracen-1-one, 10-chloroanthracen-1-one, 10-chloroanthracen-9-ol and 10-chloro-1-nitroanthracene etc.

(3) The overall rate constant for the NO_3 additions to 9-ClAnt is 9.11×10^{-13} cm^3 $molecule^{-1}$ s^{-1} at 298 K and 1atm. The atmospheric lifetime of 9-ClAnt determined by NO_3 radicals is about 0.61 hr.

Although the concentrations of ClPAHs in the atmosphere have been detected to be a lower level than those of PAHs, some may be higher than those of polychlorinated dibenzo-*p*-dioxins (PCDDs), polychlorinated dibenzofurans (PCDFs) and polychlorinated biphenyls (PCBs). To date, the investigations on the chemical transformations of ClPAHs in the atmosphere including homogeneous reactions and heterogeneous reactions have been more limited than those of other toxic persistent pollutants, such as PCDD/Fs and PAHs. However, the atmospheric reactions of ClPAHs appear to differ from those of PCDD/Fs and PAHs, and we should therefore be focused on the elucidation for the reaction mechanisms, degradation products and the capacity to undergo long-range transport of ClPAHs in the atmosphere. Thus, we can develop a comprehensive and accurate understanding of their toxic potential.

Acknowledgment

The work was financially supported by NSFC (National Natural Science Foundation of China, project Nos. 21337001, 21377073).

Supporting Information Available

The H abstraction reaction scheme of 9-ClAnt. The reaction schemes of IM1, IM2, IM3 and IM4. The isomerization unimolecular decomposition reaction scheme of the NO_3-9-ClAnt adducts. Configuration for the transition states of H abstractions from 9-ClAnt optimized at the BB1K/6-31+G(d,p) level of theory. Distances are in angstrom. The material is available free of charge via the Internet at http://pubs.rsc.org/.

References

1. K. Kakimoto, H. Nagayoshi, Y. Konishi, K. Kajimura, T. Ohura, K. Hayakawa, A. Toriba, Chemosphere, 2014, 111, 40-46.

2. A. Kitazawa, T. Amagai, T. Ohura, Environ. Sci. Technol., 2006, 40, 4592-4598.

3. K. Sankoda, K. Nomiyama, T. Yonehara, T. Kuribayashi, R. Shinohara, Chemosphere, 2012, 88, 542-547.

4. K. Sankoda, T. Kuribayashi, K. Nomiyama, R. Shinohara, Environ. Sci. Technol. 2013, 47, 7037-7044.

5. T. Ohura, Sci. World J. 2007, 7, 372-380.

6. J. Ma, Z.Y. Chen, M. H. Wu, J. L. Feng, Y. Horii, T. Ohura, K. Kannan, Environ. Sci. Technol., 2013, 47, 7615-7623.

7. J. L. Sun, H. Zeng, H. G. Ni, Chemosphere, 2013, 90, 1751-1759.

8. Y. Horii, G. Ok, T. Ohura, K. Kannan, Environ. Sci. Technol., 2008, 42, 1904-1909.

9. D. L. Wang, X. B. Xu, S. G. Chu, D. R. Zhang, Chemosphere, 2003, 53, 495-503.

10. U. L. Nilsson, C. E. Oestman, Environ. Sci. Technol., 1993, 27, 1826-1831.

11. T. Ohura, Y. Horii, M. Kojima, Y. Kamiya, Atmos. Environ., 2013, 81, 84-91.

12. T. Ohura, S. Fujima, T. Amagai, M. Shinomiya, Environ. Sci. Technol., 2008, 42, 3296-3302.

13. R. Atkinson, J. Arey, Chem. Rev., 2003, 103(12), 4605-4638.

14. I. J. Keyte, R. M. Harrison, G. Lammel, Chem. Soc. Rev. 2013, 42, 9333-9391.

15. G. P. Robert, Annu. Rev. Phys. Chem., 1983, 34, 631-656.

16. P. J. Robinson, K. A. Holbrook, Unimolecular Reactions. Wiley: New York. 1972.

17. S. H. Robertson, D. R. Glowacki, C.-H. Liang, C. Morley, M. J. Pilling,

MESMER (Master Equation Solver for Multi-Energy Well Reactions), 2008, an object oriented C++ program for carrying out ME calculations and eigenvalue-eigenvector analysis on arbitrary multiple well systems. http://sourceforge.net/projects/mesmer.

18. M. Frisch, G. Trucks, H. B. Schlegel, G. Scuseria, M. Robb, J. Cheeseman, G. Scalmani, V. Barone, B. Mennucci, G. Petersson, Gaussian 09, revision A. 02; Gaussian. Inc., Wallingford, CT 270, 271. 2009.
19. Y. Zhao, B. J. Lynch, D. G. Truhlar, J. Phys. Chem. A 2004, 108 (14), 2715-2719.
20. B. J. Lynch, D. G. Truhlar, J. Phys. Chem. A 2001, 105 (13), 2936-2941.
21. B. J. Lynch, Y. Zhao, D. G. Truhlar, J. Phys. Chem. A 2003, 107 (9), 1384-1388.
22. J. J. Zheng, Y. Zhao, D. G. Truhlar, J. Chem. Theory Comput. 2009, 5, 808-821.
23. Pilling, M. J., and Robertson, S. H. Master equation models for chemical reactions of importance in combustion, Annual Review of Physical Chemistry, 54, 245-275, 2003.
24. D. R. Glowacki, C. H. Liang, C. Morley, M. J. Pilling, S. H. Robertson, J. Phys. Chem. A, 2012, 116, 9545-9560.
25. S. H. Robertson, M. J. Pilling, L. C. Jitariu, I. H. Hillier, Phys. Chem. Chem. Phys. 2007, 9 (31), 4085-4097.
26. J. Zhou, J. W. Chen, C. H. Liang, Q. Xie, Y. N. Wang, S.Y. Zhang, X. L. Qiao, X. H. Li, Environ. Sci. Technol., 2011, 45, 4839-4845.
27. X. H. Qu, Q. Z. Zhang, W. X. Wang, Chem. Phys. Lett., 2006, 432, 40-49.
28. R. Atkinson. J. Phys. Chem. Ref. Data, 1991, 20, 459-507.

29. S. M. Zhou, J. C. Wenger, Atmos. Environ., 2013, 75, 103-112.

30. J. Sasaki, S. M. Aschmann, E. S. C. Kwok, R. Atkinson, J. Arey, Environ. Sci. Technol., 1997, 31, 3173-3179.

31. J. Dang, X. L. Shi, Q. Z. Zhang, J. T. Hu, W. X. Wang, Sci. Total Environ. 2015, 505, 787-794.

Table 1. Rate constants (cm^3 $molecule^{-1}$ s^{-1} for bimolecular reaction or s^{-1} for unimolecular reaction) for the crucial elementary reactions included in the NO_3-initiated oxidation of 9-ClAnt at 298 K and 1 atm.

Reactions	Rate constants
9-ClAnt +NO_3→NO_3-9-ClAnt	(k) 9.11×10^{-13}
9-ClAnt +NO_3→IM1	(k_1) 9.80×10^{-14}
9-ClAnt +NO_3→IM2	(k_2) 8.69×10^{-14}
9-ClAnt +NO_3→IM3	(k_3) 7.45×10^{-14}
9-ClAnt +NO_3→IM4	(k_4) 9.81×10^{-14}
9-ClAnt +NO_3→IM5	(k_5) 9.93×10^{-14}
9-ClAnt +NO_3→IM6	(k_6) 9.69×10^{-14}
IM1→IM15	3.48×10^{-20}
IM15→IM16	5.21×10^{-13}
IM16→IM17	6.92×10^{-23}
IM17→IM18	1.08×10^{-2}
IM18→P8	6.21×10^{8}
IM1→IM19	6.93×10^{-21}
IM19→IM20	5.28×10^{-13}
IM20→IM21	5.68×10^{-23}
IM23→P11	2.10×10^{8}
IM2→IM24	1.48×10^{-18}
IM24→IM25	5.23×10^{-13}
IM25→IM26	1.87×10^{-22}
IM26→IM27	2.64×10^{-1}
IM27→P8	2.31×10^{8}
IM1→IM33	3.75×10^{-9}
IM33→IM34	1.51×10^{6}
IM34→IM35	1.92×10^{4}
IM35 →P8	7.99×10^{8}
IM33→IM36	1.43×10^{6}
IM36→IM37	5.93×10^{3}
IM37→P8	5.77×10^{8}
IM57→P1	4.29×10^{-21}
IM57→P16	1.32×10^{-21}
IM59→P3	1.10×10^{-18}
IM59→P18	2.08×10^{-13}

Figure Captions

Figure 1. The NO_3 addition reaction scheme of 9-ClAnt embedded with the potential barrier ΔE (in kJ/mol, $\Delta E=E_{\text{transtion state}}-E_{\text{reactant}}$) and reaction heat ΔH (in kJ/mol, $\Delta H=E_{\text{product}}-E_{\text{reactant}}$). ΔH is calculated at 0 K.

Figure 2. The O_2 abstraction scheme of NO_3-9-ClAnt adducts embedded with the potential barrier ΔE (in kJ/mol, $\Delta E=E_{\text{transtion state}}-E_{\text{reactant}}$) and reaction heat ΔH (in kJ/mol, $\Delta H=E_{\text{product}}-E_{\text{reactant}}$). ΔH is calculated at 0 K.

Figure 3. The O_2 addition reaction scheme of NO_3-9-ClAnt adducts (IM1, IM2 and IM6) embedded with the potential barrier ΔE (in kJ/mol, $\Delta E=E_{\text{transtion state}}-E_{\text{reactant}}$) and reaction heat ΔH (in kJ/mol, $\Delta H=E_{\text{product}}-E_{\text{reactant}}$) in the presence of NO_x.

Figure 4. The unimolecular decomposition reaction scheme of IM1, IM3 and IM6 embedded with the potential barrier ΔE (in kJ/mol, $\Delta E=E_{\text{transtion state}}-E_{\text{reactant}}$) and reaction heat ΔH (in kJ/mol, $\Delta H=E_{\text{product}}-E_{\text{reactant}}$).

Figure 5. The reaction scheme of IM1 and IM6 embedded with the potential barrier ΔE (in kJ/mol, $\Delta E=E_{\text{transtion state}}-E_{\text{reactant}}$) and reaction heat ΔH (in kJ/mol, $\Delta H=E_{\text{product}}-E_{\text{reactant}}$). ΔH is calculated at 0 K.

Figure 6. The NO_2 addition reaction scheme of NO_3-9-ClAnt adducts embedded with the potential barrier ΔE (in kJ/mol, $\Delta E=E_{\text{transtion state}}-E_{\text{reactant}}$) and reaction heat ΔH (in kJ/mol, $\Delta H=E_{\text{product}}-E_{\text{reactant}}$). ΔH is calculated at 0 K.

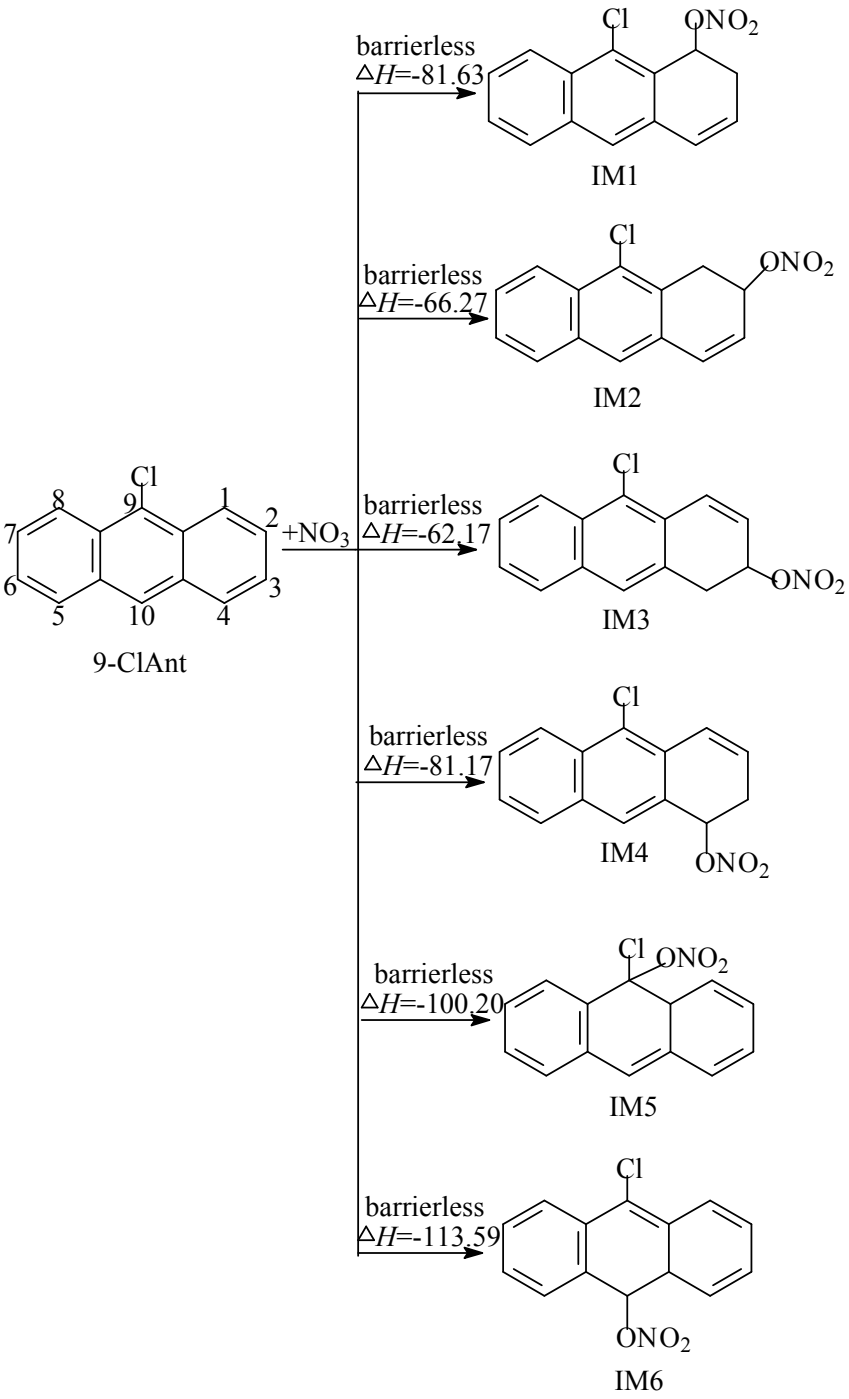

Figure 1

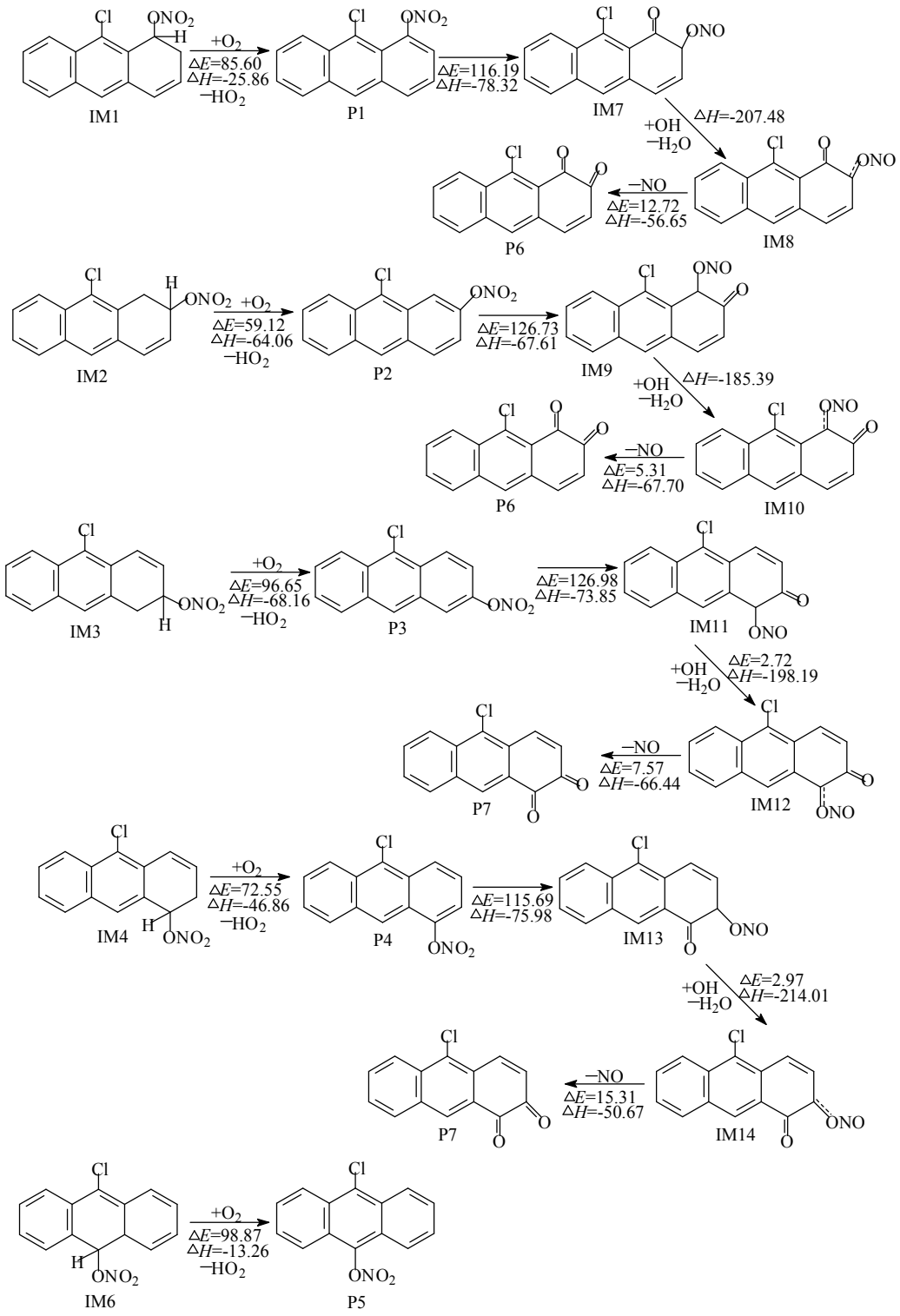

Figure 2

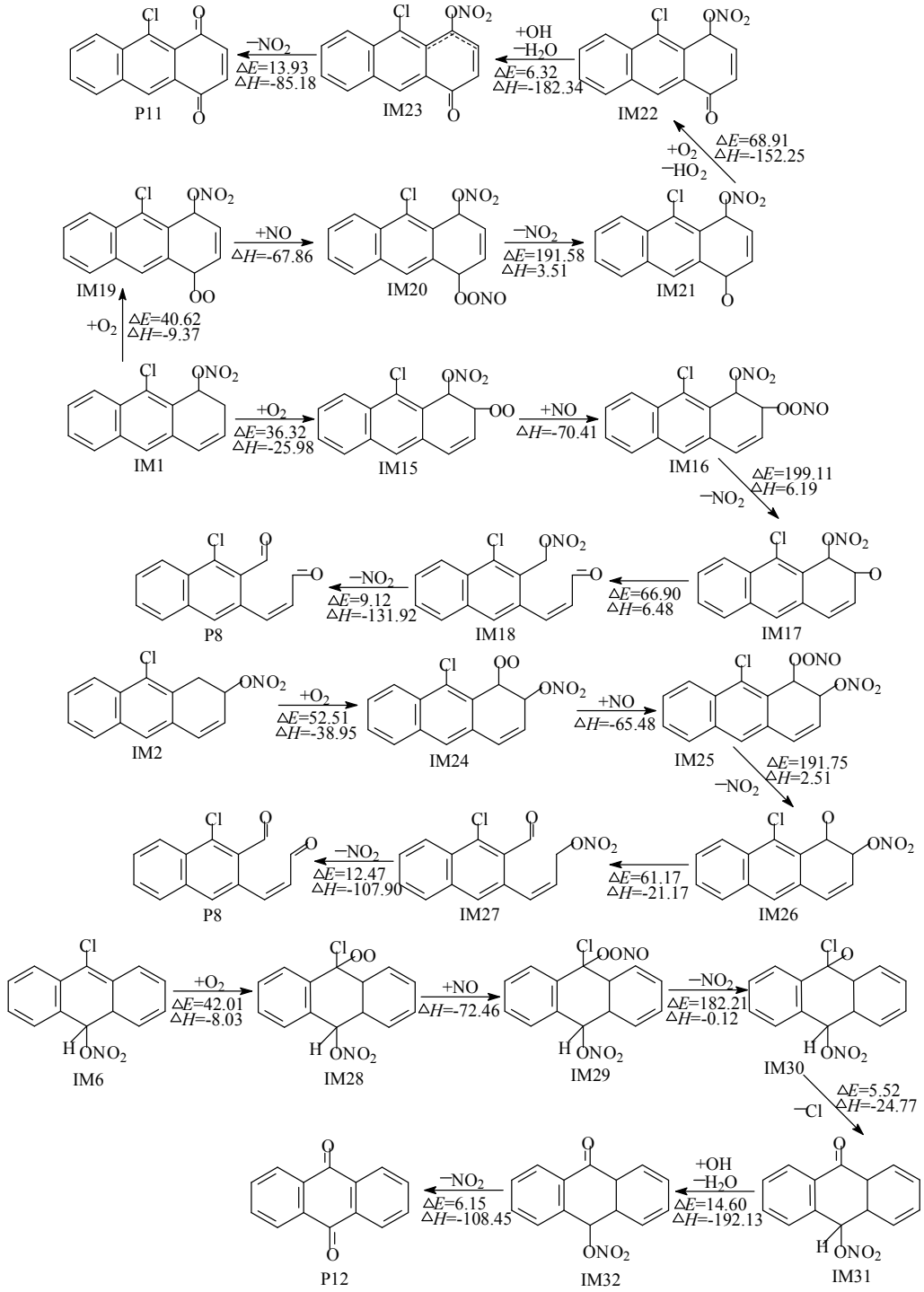

Figure 3

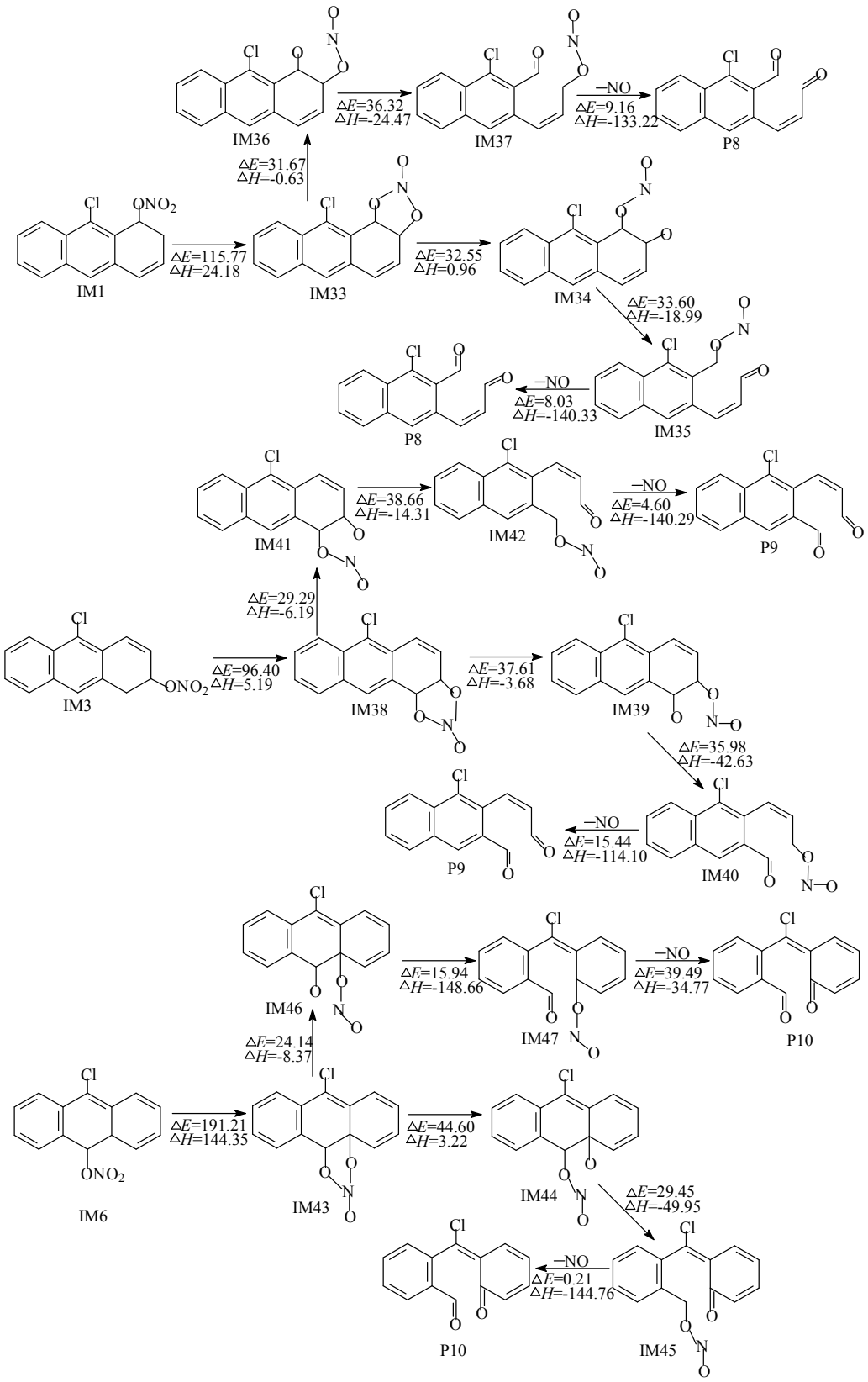

Figure 4

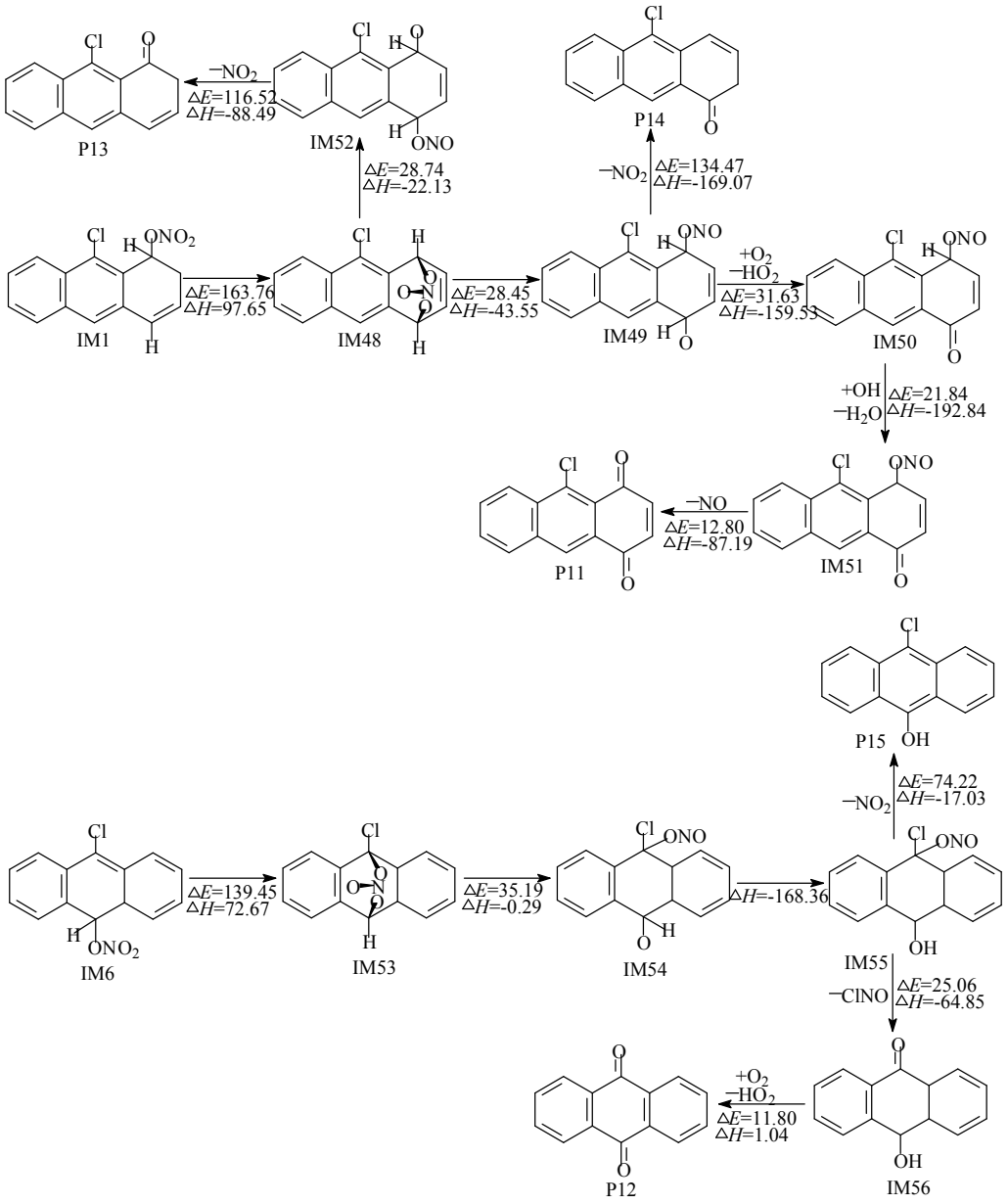

Figure 5

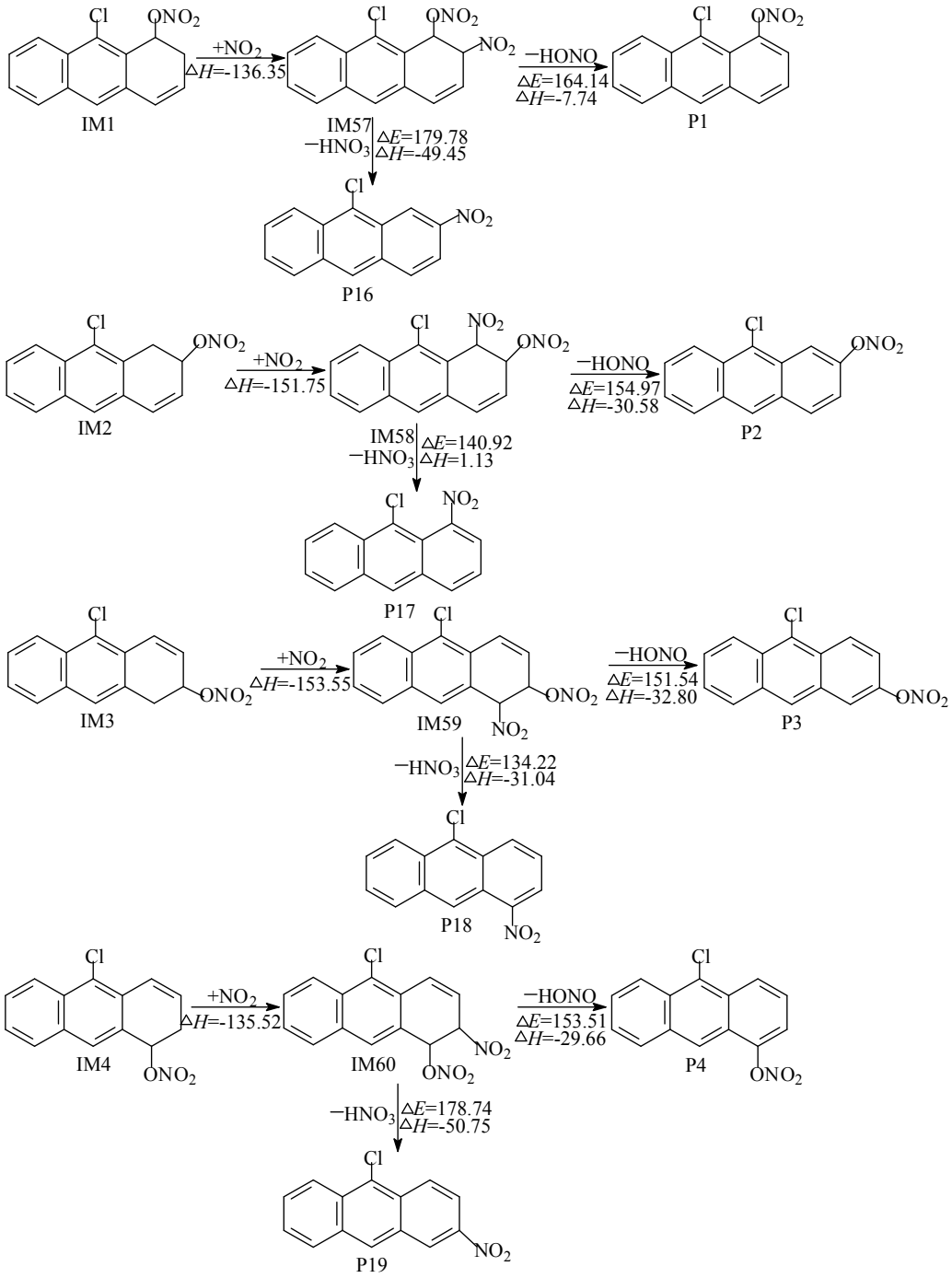

Figure 6